UNIVERSITY **POLITEHNICA** OF BUCHAREST
Faculty of Chemical Engineering and Biotechnologies
Department of Chemical and Biochemical Engineering

Nr. Decizie Senat _____/ _____________

Doctoral Thesis

ABSTRACT

Sorption processes with sorbents from natural products

Author: Eng. **Shaalan Bdaiwi AHMED**
PhD Supervisor: Prof. PhD. Eng. Tănase DOBRE

Doctoral Committee

Function	Title, Complete Name	Affiliation
President	Prof. PhD. Eng. Dănuț-Ionel VĂIREANU	University POLITEHNICA of Bucharest
PhD Supervisor	Prof. PhD. Eng. Tănase DOBRE	University POLITEHNICA of Bucharest
Reviewer	Assoc. Prof. PhD. Eng. Iuliana DELEANU	University POLITEHNICA of Bucharest
Reviewer	Prof.PhD. Eng. Ioan MĂMĂLIGĂ	University GHEORGHE ASACHI of Iași
Reviewer	Prof. PhD. Eng. Alexandru OZUNU	University BABEȘ-BOLYAI of Cluj Napoca

Bucharest, 2022

Thesis Content

CHAPTER 4.Models at particle level in adsorption of heavy metals on vegetable sorbents

Notă: Rezumatul tezei este deschis de o introducere în care se prezintă, la modul general, conținutul fiecărui capitol, cu marcarea unor aspecte ce dau originalitate lucrării. Se continuă apoi cu prezentarea unor paragrafe din teză care conțin elemente proprii. Aceste paragrafe sunt preluate în forma lor din teză cu specificarea localizării lor în teză. Ultima parte a rezumatului conține concluziile tezei și realizările de diseminare a rezultatelor tezei.

Note: The thesis summary is opened by an introduction in which the content of each chapter is presented, in a general way, with the marking of some aspects that give the work originality. It then continues with the presentation of some paragraphs from the thesis that contain their own elements. These paragraphs are taken in their form from the thesis, with the specification of their location in the thesis. The last part of the summary contains the thesis conclusions and the achievements of disseminating the results of the thesis.

Keywords: adsorption, heavy metals, wastewater, mass transfer, intensification, ultrasounds

Introduction

The sorption processes in which sorbents from natural products are used are found in many industrial applications. Now they have an actual development field, determined by the intense promotion of sorbents from vegetable materials, more or less processed. The thesis focuses on the problem of promoting of sorption processes with sorbents from natural products as application for removing heavy metals from wastewater. In this sense, it starts with the presentation of water pollution with heavy metals, showing what are the pollution sources and what effects, on the environment and health, are due to the presence of most of the heavy metals in the environment (water, air, soil). Then it continues with presentation of available solutions for heavy metals (HM) removal from wastewater, insisting on chemical methods and on those based on their (HM) adsorption on sorbents from residual plant materials. The thesis has as its application a more complete characterization of the use of sorbent obtained from vegetable residues from hazelnut shells for the processing of wastewater containing Pb(II) and Cd(II), heavy metals extremely dangerous for the environment. As the thesis is strongly focused on the chemical engineering aspects of the liquid-sorbent interphase transfer of HM pollutants, special attention is paid to the statics and dynamics of this process. Thus, the interphase equilibrium models and the investigation procedures, specific to the identification of their parameters, are presented. Based on experimental research of fixed bed sorption of Pb(II) and Cd(II), from wastewater, onto HS particles, at the end of chapter 2, the identification of Freundlich and Langmuir equilibrium models parameters is presented,. The data and the analytical expression regarding the simultaneous transfer equilibrium of Pb(II) and Cd(II), from wastewater, to HS particles are interesting here. Considering the interest of interphase mass transfer research for using intensive methods, of great technological value, it was decided to use in this thesis and to promote cases of sorption in the ultrasonic field. First case of this solution is developed under the title Ultrasonic intensification of Pb(II) removal by biosorption on HS. The kinetic model of interphase transfer in sorption of a species such as HM at particle level is given an important attention, thus mentioning, and discussing the case of 7 possible models. They are differentiated by the competition between surface and pore diffusion and linear or non-linear interaction kinetics, which accompany the fixation of the species to the active sites in the sorbent. The extensive case study from chapter 4 brings, for the first time, as results, values of kinetic constants of species sorption and desorption and of diffusion coefficients, for Pb(II) and Cd(II) removal sorption by on HS particles in gravitational and ultrasonic. Knowing that in applications the fixed sorbent bed sorption is the most used, in chapter 5 this problem is analyzed, highlighting the importance of identifying and characterizing of sorption breakthrough curves.

For non-competitive adsorption of Pb(II) and Cd(II) from wastewater on HS, the breakthrough curves can be characterized with some semi-empirical models, from the literature. For competitive adsorption, however, complicated phenomenological models must be used, as it shown and exemplified, by a concrete case, at the end of chapter 5. In the problem of multi-level characterization of Pb(II)m and Cd(II) sorption, from wastewater on HS particles sorbent, statistical models and phenomenological models in numerical expression are used. The development of thesis is supported by a large number of bibliographic references, that are presented in each chapter.

1.2. **Heavy metals in Mendeleev Table: Common elements and differences** (6-8, Cap.1)

If we tried a definition of what heavy metals are then this would be: *The metals which have higher density or higher atomic mass are known as heavy metals.* But one thing I want to tell you that you may find a different definition of heavy metals in metallurgy, physics as well as chemistry. Here is why. In metallurgy, researchers define heavy metals on the basis of density. In physics, they may use atomic numbers for defining heavy metals. In chemistry, chemists and chemical engineers are concerned with the chemical properties of heavy metals for defining them. So, there is a research work still going on for the specific definition and classification of heavy metals.Now the question is: How can we come to know which metals are heavy metals?

Well, many researchers use the common criteria that **if the metals have the density of more than 5000kg/m³, then they are likely to be known as heavy metals.** On the basis of these criteria, the heavy metals are marked in Periodic Table as in Figure 1.1.

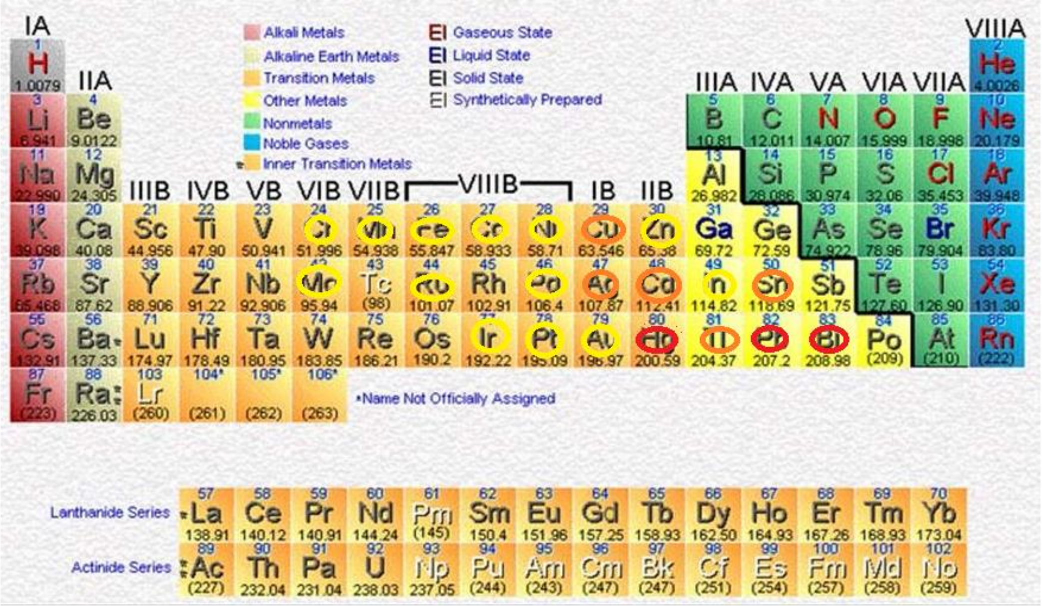

Figure 1.1 Heavy metals in Mendeleev Table and the most dangerous of them

Taking into account the above definition for heavy metals, we discover in Mendeleev Table that all species named transition metals (orange marked in Fig. 1.1) and all species from class others, metals (yellow marked in Fig.1.1) obtain qualification as heavy metals. According to their density and those of their compounds, according to their own toxicity, according to the toxicity of their compounds inclusively of those insoluble in water, according to the effects on the health of living organisms, we find:

i) Heavy metals of first class characterized by those that all mentioned classification criteria have maximum values (density over 9500 kg/m3, metal with proper toxicity, all chemical species of those metals water's soluble and insoluble show toxicity, very strong toxic effect on living systems). We have here Hg, Pb, Bi, which are toggled in Fig 1.1 with red color.

ii) Heavy metals of second class characterized by those that all mentioned classification criteria have middle values (density in the range 6500 -10500 kg/m^3, low proper toxicity of metal, we find that chemical species of those metals, water soluble and insoluble, show moderate or low toxicity, strong toxic effect on living systems). We have here Cu, Ag, Cd, Sn, Tl and in Fig.1.1 it has orange toggle.

iii) Heavy metals of third class characterized by those that most of mentioned classification criteria have middle or low values (density in the range 6500 -22400 kg/m^3, very low or absent metal proper toxicity, we find that chemical species of those metals, water soluble and insoluble, with low toxicity, moderate toxic effect on living systems). We have here Cr, Mn, Fe, Co, Ni, Zn, Mo, Rd, Pd, Ir, In, Pt, Au, and Po. In Fig.1.1 we marked these heavy metals with a yellow toggle.

This classification, concentrated also in Table 1.1, must be regarded as non-exhaustive. In this sense, respect to criterion regarding effect on living systems we show that only a relatively small number of heavy metals such asCadmium, Copper, Iron, Cobalt, Zinc, Mercury, Vanadium, Lead, Nickel, Chromium, Manganese, Molybdenum, Silver, and Tin as well as the metalloids Arsenic and Selenium are associated with environmental, plant, animal, or human health problems.Lead and Cadmium, which was selected as heavy metals used in this thesis, are among the 20 metals classed as hazardous and half of these are released into the environment in proportions that pose a threat to human health [9].Our notes from Table 1.1 take into account that the bodies of living systems, to operate properly, need certain heavy metals like iron, copper, zinc, magnesium, manganese and others. Therefore, small amounts of these elements are found in nature and are essential to our health, but exposure to excessive levels of any of these elements can have acute or long-term harmful effects [10-12].

Table 1.1 A tentative for classification of heavy metals upon environmental effect

No.	Z	Heavy metal	ρ kg/m^3	Metal toxicity*	Compounds toxicity*	Effect on living systems*
1	80	Mercury (Hg)	13550	10	10	10
2	82	Lead (Pb)	11350	9	10	9
3	83	Bismuth (Bi)	9750	8	9	8
4	29	Copper (Cu)	8960	5	7	7
5	47	Silver (Ag)	10500	4	8	8
6	48	Cadmium (Cd)	8650	7	8	8
7	50	Tin (Sn)	7310	6	7	6
8	81	Thallium (Tl)	9320	6	7	8
9	24	Chromium (Cr)	7190	5	7	7
10	25	Manganese (Mn)	7430	5	7	6
11	26	Iron (Fe)	7860	4	6	6
12	27	Cobalt (Co)	8900	4	5	6
13	28	Nickel (Ni)	8900	2	5	6
14	30	Zinc (Zn)	7130	2	5	5
15	42	Molybdenum (Mo)	10220	2	5	5
16	45	Rhodium (Rh)	12410	1	5	5
17	46	Palladium (Pd)	12020	1	4	5
18	49	Indium (In)	7310	1	4	5
19	77	Iridium (Ir)	22400	1	4	5
20	78	Platinum (Pt)	21450	1	3	4
21	79	Gold (Ag)	19320	1	2	2
22	84	Polonium (Po)	13670	3	-	6

* **Scoring on a scale of 1 to 10 according to our proper opinion**

For many decades, heavy metal water pollution has been a major source of worry due to the high level of toxicological danger it poses to human health, the environment, and agriculture. Toxic heavy metals tend to accumulate in living organisms due to their non-biodegradability and persistence, causing a wide range of diseases and disorders [13,14,15]. So, because of the toxicity, persistence, and bioaccumulative nature of these materials, research on heavy metals in the ambient is an important part in environmental research.

2.3.4 Equilibrium of two components adsorption processes: Case of simultaneous sorption of Pb^{+2} and Cd^{+2}on hazelnut shell (63-65, Cap.2)

In this paragraph we bring data obtained at simultaneous Pb(II) and Cd(II) sorption in a hazelnut shells sorbent as fixed bed of particles with diameter 0.7-1 mm. The working procedure for fixed bed sorption results from the work [117]. The experimental data, here given, were obtained when it operates with a flow rate of 1.4 ml/min and a 0.07 m bed height. The bed was from HS particles with 0.76 -1 mm in diameter. The total concentration of Pb(II) and Cd(II) in the liquid phase, at the bed input was 25 mg/l, 50 mg/l, 75 mg/l and 100 mg/l, respectively. In this concentration, half was Pb (II) and half was Cd (II).

Figure 2.9 concentrates our eight breakthrough curves. The four steep procedure, above used for single component sorption, was assigned for processing of breakthrough curves from figure 2.8 to q_e vs. c_e dependency. We show that c_0 concentration of bath species are given in figure 2.9. And at the same time we remind the 4 steps procedure with for q_e vs. c_e link: i) read the Excel data of breakthrough curve, ii) use Excel data to establish the value of integral from relation (2.31), iii) establish q_{total} and q_e values according with relations (2.32) and (2.33); iv) assume correspondence q_e to c_e. Table 2.5 concentrates the result of q_e vs. c_e dependency.

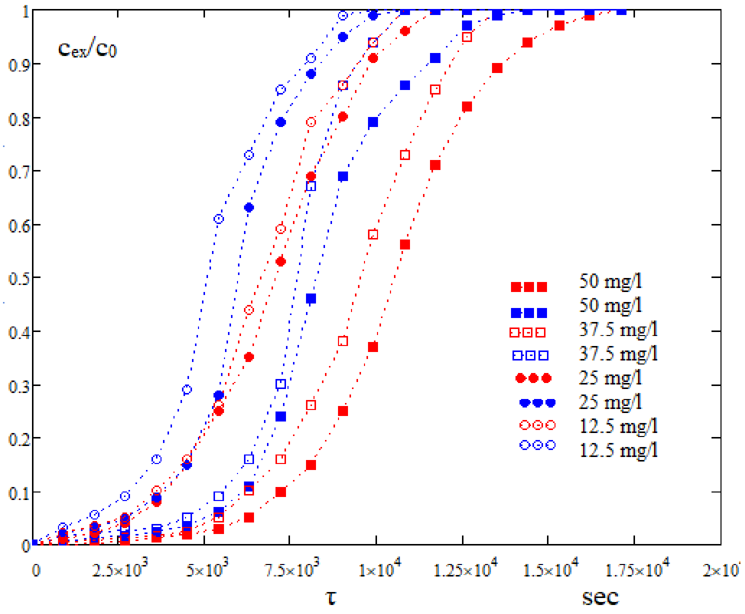

Figure 2.9. Breakthrough curves for simultaneous Pb(II) and Cd^{+2} adsorption on fine particles of hazelnut shell at pH=6 , t= 25^0C , h (L) = 0.07 m and Q=1.4 ml/s

Table 2.5 Experimental results equilibrium data for simultaneous Pb(II) and Cd (II) sorption on HS processed particles with 0.7 – 1 mm

No.	Conditions	c_{T0} mg/l	$c_0 = c_e$ mg/l	q_{ePb} mg/g	q_{eCd} mg/g
1	t= 25 ^{0}C Fixed bed h=0.07 m Q_l = 1.4 ml/s d_p – 0.7 -1 mm	25	12.5	10.61	8.34
2		50	25	17.79	13.76
3		75	37.5	22.43	18.88
4		100	50	25.13	19.10

The particularization of the Freundlich model (2.24), for the case of simultaneous Pb (II) and Cd (II sorption on HS particles, is described by relations (2.41) and (2.42). Their applicability to concrete case is related to the fact that it is not known what value have c_{eCd} when c_{ePb} is chosen. We considered a correction of these relations, as it is shown by relations (2.43) and (2.44), where α and β can be determined by simultaneous minimizing of mean square deviations between calculated and experimental values for the dependencies q_{ePb} vs.c_{ePb} and q_{eCd} vs. c_{eCd}:

$$q_{ePb}(c_{ePb}) = \frac{K_{Pb}c_{ePb}^{n_{Pb}}}{1+\left(K_{Pb}+K_{Cd}c_{eCd}^{n_{Cd}-n_{Pb}}\right)} \qquad (2.41)$$

$$q_{eCd}(c_{eCd}) = \frac{K_{Cd}c_{eCd}^{n_{Cd}}}{1+\left(K_{Cd}+K_{Pb}c_{ePb}^{n_{Pb}-n_{Cd}}\right)} \qquad (2.42)$$

$$\mathrm{q_{ePb}}(\mathrm{c_{ePb}}) = \frac{\alpha \mathrm{K_{Pb}} \mathrm{c_{ePb}^{n_{Pb}}}}{1+\beta \mathrm{K_{Cd}} \mathrm{c_{ePb}^{n_{Cd}-n_{Pb}}}} \qquad (2.43)$$

$$\mathrm{q_{eCd}}(\mathrm{c_{eCd}}) = \frac{\alpha \mathrm{K_{Cd}} \mathrm{c_{eCd}^{n_{Cd}}}}{1+\beta \mathrm{K_{Pb}} \mathrm{c_{eCd}^{n_{Pb}-n_{Cd}}}} \qquad (2.44)$$

A similar procedure with γ and δ instead of α and β was considered to express this equilibrium. Relationships (2.45) and (2.46) express this situation.

$$q_{ePb}(c_{ePb}) = \frac{\gamma q_{mPb} b_{Pb} c_{ePb}}{1+\delta(b_{Pb}+b_{Cd})c_{ePb}} \qquad (2.45)$$

$$q_{eCd}(c_{ePb}) = \frac{(\gamma-\delta) q_{mCd} b_{Cd} c_{eCd}}{1+\delta(b_{Pb}+b_{Cd})c_{ePb}} \qquad (2.46)$$

With K_{Pb}, n_{Pb}, K_{Cd}, n_{Cd} from relations (2.33) and (2.34), with q_{mPb}, b_{Pb}, q_{mCd}, b_{Cd} from relations (2.35) and (2.36) and with experimental data from table (2.5) simultaneous minimizing of mean square deviations between calculated and experimental values for the dependencies q_{ePb} vs. c_{ePb} and q_{eCd} vs. c_{eCd} was put in work, in order to identify the best values of α, β, γ and δ. Table 2.6 contains identified values for α, β, γ and δ and give a comparison between computed and experimental values of dependencies q_{ePb} vs. c_{ePb} and q_{eCd} vs. c_{eCd} .

$$q_{ePb} = 0.806c_{ePb}^{0.806} \qquad (2.33)$$

$$q_{eCd} = 1.662c_{eCd}^{0.554} \qquad (2.34)$$

$$q_{ePb} = \frac{0.575\ c_{ePb}}{1+0.008897c_{ePb}}\ , \quad R^2 = 0.992 \qquad (2.35)$$

$$q_{eCd} = \frac{0.712c_{eCd}}{1+0.028c_{eCd}}\ , \quad R^2 = 0.979 \qquad (2.36)$$

Table 2.6. A short comparison between computed and experimental values of dependencies q_{ePb} vs. c_{ePb} and q_{eCd} vs. c_{eCd}

No.	Parameters	c_{T0} mg/l	$c_0 = c_e$ mg/l	q_{ePb} mg/g exp	q_{eCd} mg/g exp	q_{ePb} mg/g (2.43)	q_{eCd} mg/g (2.44)	q_{ePb} mg/g (2.45)	q_{eCd} mg/g (2.46)
1	α = 1.5 β = 0.08 γ= 1.5 δ = 0.45	25	12.5	10.61	8.34	8.65	9.03	9.23	8.57
2		50	25	17.79	13.76	15.28	12.99	15.74	14.62
3		75	37.5	22.43	18.88	21.03	16.02	20.59	19.12
4		100	50	25.13	19.10	26.95	18.65	2483	21.59

Those from Table 2.6 show that the proposed procedure that modify the customization of the Freundlich and Langmuir model for the simultaneous adsorption of two components, here Pb(II) and Cd(II) species on HS particles, gave good results. It should be noted, however, that in many cases this problem of multicomponent sorption equilibrium is treated individually for each species, using a distribution coefficient.

3.5. Ultrasound enhanced removal of lead from wastewater by hazelnut shell bio sorbent– an experimental design methodology (94-106, Cap. 2)

Inside of chapter 2 we showed that the adsorption processing using ultrasonic field a very good of the interphase solute transfer enhancement is achieved. In the previous paragraph showed that the adsorption statistical modeling by mean of experiments programming is a solution to have maximum information with minimum experimental effort. The present paragraph unites these two aspects on the concrete case of Pb (II) removal from the polluted water, using, as a sorbent, hazelnut shell particles. The chapter is entirely based on the paper published by Bdaiwi Ahmed et all. in 2018 [47]. So, we use here the most part of this published paper.

3.5.1. Introduction on problem of heavy metals removal from wastewater

Heavy metals, occurring in municipal wastewater, are considered “special components” and although they might not be the direct target of treatment, they have a significant impact on both biological wastewater treatment, and on the receiving water bodies [48]. Because, unlike the biodegradable matter, heavy metals are actually accumulating in the living tissues causing serious illnesses even at very low dosages, the World Health Organization (WHO) lowered over the years the permissible limits of metals in drinking water [49]. Among all, lead is considered as one of the most hazardous heavy metals, and while its typical medium concentration in wastewater is around 60 mg/L, the guideline value in drinking water is 10 µg/L. However, it must be noted that this value is maintained and considered as provisional since lead is occurring from various sources (including pipelines) some difficult to control, but also because the treatment performance and analytical achievability make very difficult to reach lower concentration values.Many techniques have been investigated for the removal of Pb(II), from the conventional precipitation [50] to new membrane separations [51],but high operational costs and more important, the ineffectiveness at low concentration, limited their applicability. In contrast, adsorption processes, widely investigated, proved to be both efficient and in some cases inexpensive, as agricultural, and other wastes were used as renewable, effective, low-cost absorbents [52 – 55]. Hazelnut shell (HS), a food industry lignocellulosic waste, quite abundant in countries like Turkey and Italy is currently used as fuel for its high calorific value. In many researches it was investigated as material for the preparation of activated carbon due to its high carbon and low ash content [56]. But because of high costs associated to activated carbon preparation and usage, the HS, among other low-cost materials, despite lower sorption potential, was also tested as biosorbent for heavy metals and dyes [57 – 59]. The overall objective of this study is to prove the effectiveness of ultrasounds-assisted adsorption (US-AA) of Pb (II) onto HS. The goal is to take the benefits of the mechanical and chemical effects of ultrasounds (US) to enhance mass transfer rate. Thus, the effect of US on the equilibrium and kinetics of lead biosorption onto hazelnuts shell was investigated using Response Surface Methodology (RSM) and Central Composite Design to determine the optimal conditions for the process.

3.5.2. Experimental procedures and equipment

Materials: The shells of hazelnut purchased from the market in Iraq region were used in this study. Before usage they were washed several times with distilled water and dried. After, the shells were grounded using a knife mill and sieved. The fraction between –0.5 and +0.63 mm was used for all experiments. The stock solution, with a concentration of 1000 mg/L Pb(II), was prepared using analytical reagent grade $Pb(NO_3)_2$ supplied by Merck. Working solutions, of specified concentrations, were prepared from the stock solution by dilution with distilled water. When needed, the solutions pH was adjusted using 0.1N NaOH and 0.1N HCl solutions and measured with a digital pH-meter.

Adsorbent characterization: The microscopic morphology and chemical composition of grounded particles were explored using a FEI Quanta Inspect F Scanning Electron Microscope (SEM), operated at 25 kV, equipped with energy-dispersive X-ray Spectroscopy (EDS). Since the specimens are not conductive, they were subjected to DC sputtering in order to deposit a thin and continuous layer of gold on the surface. Both Secondary Electron (SE) and Back-Scattered Electron (BSE) imaging modes were employed. Fourier Transform Infrared (FT-IR) spectra of the particles were recorded in an IR Spectrometer Nicolet 6700 - Thermo Scientific, connected to an attenuated total reflection, ATR accessory (Zn/Se crystal). For each region, a series of spectra were recorded, and every spectrum consisted of 125 co-added spectra at a resolution of 4 cm^{-1}, in the range from 4000 to 600 cm^{-1}.

Experimental design and optimization of ultrasound-assisted adsorption (US-AA)

Apparatus: The set-up consisted in a 500-Watt net power output and 20 kHz frequency Ultrasonic Processor VCX500 VibraCell Sonics USA, with a 19 mm diameter solid type, high intensity probe (max. amplitude 75 µm) suitable for medium volume applications. The temperature was controlled and maintained by water circulating from a thermostatic bath.

Samples were taken from the flask at predetermined time intervals, and adsorbent was immediately removed by filtration. The residual Pb(II) concentration was determined in the filtrate using an Agilent ICP Triple Quad (ICP-QQQ), equipped with an octupole collisionreaction cell positioned between two quadrupole mass filters and autosampler. The samples were diluted using nitric acid 65% Suprapur® supplied by Merck Millipore. The instrument was operated in single-quad mode.

Adsorption experiments: All US-AA experiments were carried out at optimal conditions determined in a preliminary experimental study, as will be briefly presented in Results and Discussions section: pH=5 and an adsorbent dosage 0.5 g sieved shell particles per 50 mL solution. Each experiment was conducted in batch conditions, using 250 mL solution. The amplitude for each experiment was set at 30%. Solution concentration, adsorption time and temperature were modified according to Box-Behnken Design (BBD) matrix. The STATISTICA statistical package software trial version (Stat Soft Inc., Tulsa, USA) was used for experimental design analysis and data processing.

Equilibrium experiments: For these experiments, the working solutions concentration varied from 20 mg/L to 200 mg/L. The rest experimental conditions were maintained the same as in the case of US-AA experiments (pH=5, adsorbent dosage 0.5 mg per 100 mL solution, amplitude 30 %). The amount of Pb(II) adsorbed per unit mass of biosorbent at equilibrium was calculated using the following equation:

$$q_e = (C_0 - C_e) \cdot V/m \qquad (3.87)$$

Adsorption isotherms as expression of molecules distribution between solid and liquid phases at were developed and described using Langmuir and Freundlich models (the most used by literature), as described in Chapter 2 and resumed here in Table 3.8.

Table 3.8 Adsorption isotherms for paper data processing [60,61]

Isotherm	*Linear form*		*Characteristics and applicability*
Langmuir	$\frac{1}{q_e} = \frac{1}{q_m \cdot b \cdot C_e} + \frac{1}{q_m}$	(3.88)	adsorption on homogeneous surface monolayer adsorption
Freundlich	$log q_e = log K_F + \frac{1}{n} \cdot log C_e$	(3.89)	earlier empirical equation exponential distribution of active centers adsorption on heterogeneous surface

3.5.3 Results and discussion

Characterization of adsorbent. HS is a lignocellulosic material with average 30% cellulose, 30% lignin and 11% hemicelluloses, depending on provenience. For a better understanding of US effect on the microstructure morphology SEM investigations were performed. In Fig 3.4 there are presented SEM and EDS images of HS particles before and after adsorption. All SEM images illustrate lumpy granular structure characteristic to HS as observed by others [62,63]. However, there is noticeable the difference between the original and the Pb loaded adsorbent material. Because of grinding, the original HS presents a leafier, irregular structure while, due to US, the treated particles surface is cleaned with no gaps or rugosities.

EDS graphs, used only as qualitative test, indicate Pb(II) presence in all samples, except the initial one. It can also be seen that the initial solution concentration is also an important factor in adsorption process. Thus, for low Pb(II) solution concentration the metal distribution can be characterized as discrete dots, but when the concentration increased the metal deposition followed a certain pattern in direct correlation with adsorbent chemical structure, with larger conglomerations as a result of combined effect of the three different binding mechanisms already reported: simple adsorption, ion exchange and formation of complexes [64].

FTIR spectra of HS particles before adsorption and after adsorption at 20 ^{0}C for an initial solution concentration of 200 mg/L Pb(II) are presented in Fig. 3.5. Only minor differences are observed between initial spectrum and the spectrum after adsorption. A major peak located at 3443 cm^{-1} on the initial spectrum could be attributed to –OH stretching vibration and the peak at 2886 cm^{-1} is due to –CH_2 stretching vibrations. In the spectrum of HS particles after adsorption, these peaks are shifted at 3396 cm^{-1} and at 2926 cm^{-1} and are more visible indicating a possible participation of these functional group in Pb(II) binding [65]. The bands at 1612 cm^{-1} (shifted at 1610 cm^{-1} in the HS particles spectrum after adsorption) and at 1515 cm^{-1} (shifted at 1510 cm^{-1} in the HS particles spectrum after adsorption) could be assigned to C=C stretching of aromatic ring in lignin. The peak at 1036 cm^{-1} in the HS particles spectrum after adsorption, which could be attributed to C-O stretching of primary alcohols and carboxylic acids [64] becomes very sharp in comparison with the HS particles spectrum before adsorption. FTIR spectra of the adsorbent used in these experiments confirm that it has a complex composition and present many functional groups which could participate at Pb(II) bending during adsorption.

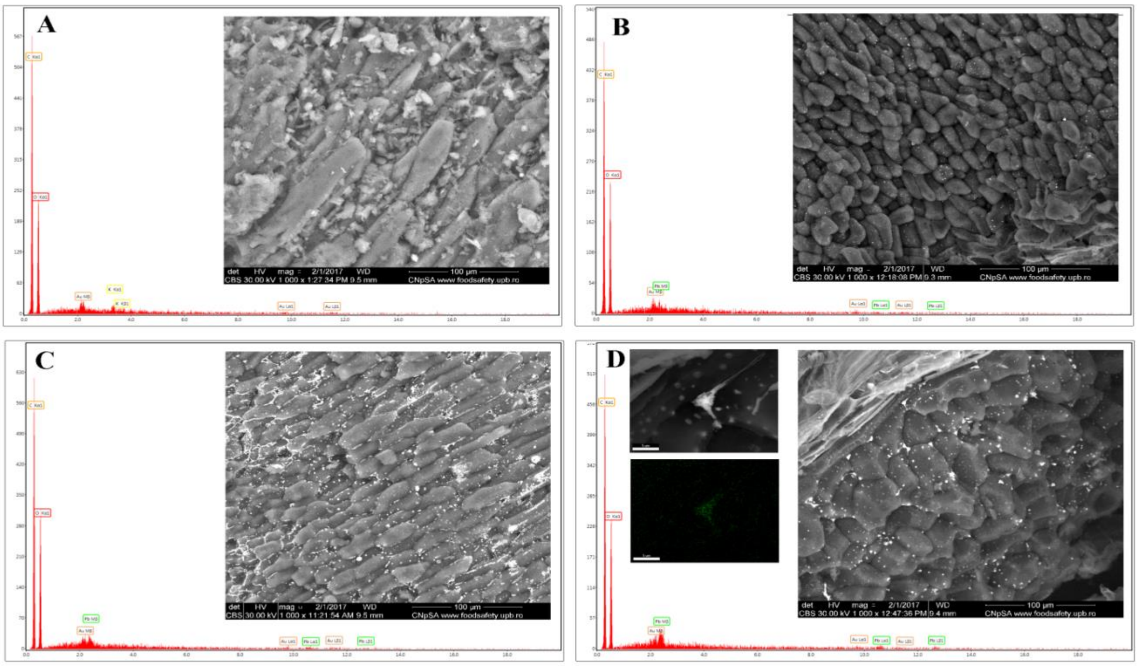

Figure 3.4 SEM-EDS of (A) unused HS and HS after US-assisted adsorption at 20 ºC, (B) C_0 = 20 mg/L, (C) C_0 = 50 mg/L, (D) C_0 = 200 mg/L, including a distribution map of Pb (II)

Optimization of Pb(II) adsorption on HS – preliminary investigations: The main objective of this study was to increase adsorption performance, as a possible industrial method for the removal of Pb(II) from wastewater. Previous investigations regarding the adsorption of Pb(II) using hazelnut shells and other low-cost, eco-friendly biosorbents, indicate a long, or very long, time to achieve a good biosorption efficiency, from one or two hours until 24 hours or even more [65]. Also, it was found that application of US irradiation, due to production of acoustic cavitations, has a positive effect, accelerating mass transfer processes by various mechanisms [66]. Therefore, the US-assisted biosorption was considered in this study, to achieve fast and efficient Pb(II) removal. Two distinct sets of preliminary experiments were conducted: 1- Classical batch adsorption experiments with mechanical stirrer to determine an initial range of operating parameters; 2- A preparatory experiment, to evaluate necessary time to establish the equilibrium in ultrasound-assisted adsorption.

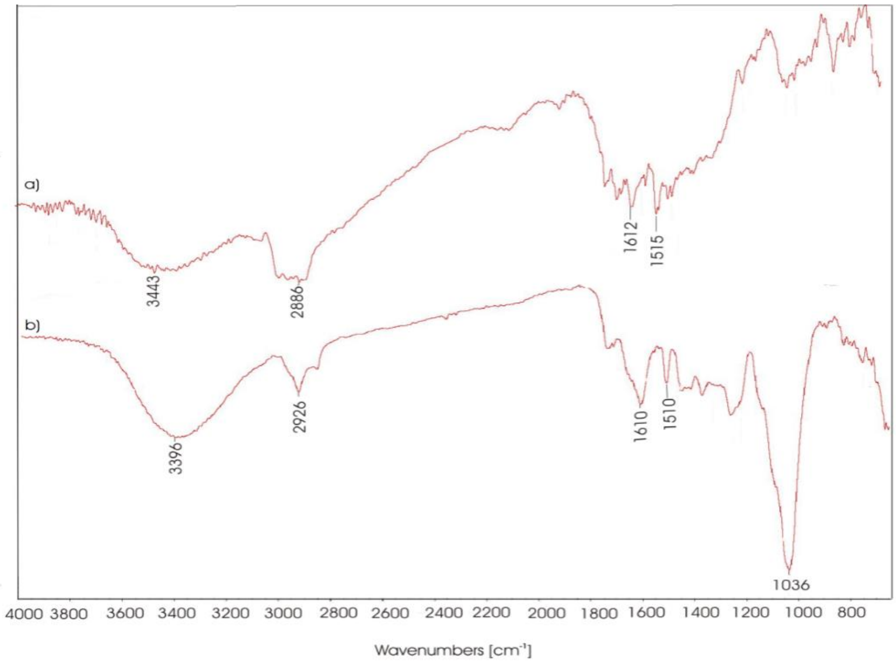

Figure 3.5 FTIR spectra of HS: a) particles before adsorption and b) particles after Pb (II) adsorption

The performance of the biosorption was expressed as removal efficiency (R), calculated according to the following the relation (3.90)

$$R(\%) = (C_0 - C_r)/C_0 \cdot 100 \qquad (3.90)$$

There must be mentioned from the beginning that, since the possible application is in the field of wastewater treatment, Pb(II) concentration of solution in the preliminary experiments was maintained at a rather low value: 50 mg/L. Regarding the contact time, as reported by other previous researches [64], it was considered that 180 min are enough to achieve saturation. Polyphenolic compounds with hydroxyl groups (like lignin) are considered the active sites responsible for Pb(II) removal from aqueous solutions [64], thus, because of this specific composition, the main parameters investigated were the pH, adsorbent dosage and contact time. The particles dimension was maintained in the range 0.5 -0.63 mm for an easy, low energy-consumption subsequent separation of the solid particles (on industrial scale perspective). The results of Set 1 of experiments, not presented here, indicate a good removal efficiency for pH around 4 – 5, and poor efficiency at lower or higher pH values, in good agreement with previous reports [67]. As expected, the surface charge of sorbent is pH dependent and influences the adsorption. Also, the optimum adsorbent dosage was concluded at 0.5 mg for each 50 mL of solution. Increased dosage did not significantly improve the adsorption. In a more conservative approach, the necessary time to evaluate the removal efficiency was investigated in two experiments: a silent experiment (classic stirred batch) and an ultrasound assisted one, each with a duration of 220 min, in the same conditions (Set 2): pH 5, initial solution concentration 50 mg/L, temperature 25 ºC. The results indicated that the adsorption assisted by US was very rapid compared to the silent one. Furthermore, a longer contact time lead to a slight decrease of removal efficiency because of particles ruptures under the US effect, as observed visually.

Pb(II) adsorption on HS – optimization using Response Surface Methodology (RSM): Considering the results and the conclusion of Set 1 and Set 2 experiments, the conditions for the US-AA experiments were set as indicated in the Experimental Section. This investigation aims to determine the optimum conditions for US-AA of Pb(II) by HS, by three levels, three factorial BBD experiment. This methodology allows the formulation of a quadratic equation to describe the process:

$$Y = \beta_0 + \sum \beta_i x_i + \sum \beta_{ii} x_i^2 + \sum \beta_{ij} x_i x_j \qquad (3.91)$$

The efficiency of the model, generated after the regression analysis of the response, was tested by ANOVA and Fisher's F-test. The interactions between variables were also represented using three-dimensional response surface plots. The process factors are: contact time (X_1), initial solution concentration (X_2) and solution temperature (X_3). It is clearly that they are independent. The three factor levels are –1 (low), 0 (central point) and +1 (high). The dependent variable is considered the removal efficiency. In Table 3.9 there are presented the levels and code of variables selected for BBD.

Table 3.9 Experimental factors and levels

Factors	*Levels*		
	–1	0	+1
X_1 (time, min)	4	7	10
X_2 (initial Pb(II) conc., mg/L)	20	50	80
X_3 (temperature, ºC)	20	30	40

Table 3.10 Box-Behnken experimental design matrix of independent variables and the corresponding experimental and predicted values for removal efficiency (Y_1)

Run	X_1	X_2	X_3	Y_1 experimental (%)	Y_1predicted (%)
1	-1	-1	0	91.62	91.62
2	1	-1	0	92.18	92.08
3	-1	1	0	96.68	96.78
4	1	1	0	97.07	97.07
5	-1	0	-1	96.28	96.00
6	1	0	-1	96.32	96.13
7	-1	0	1	93.91	94.09
8	1	0	1	94.43	94.71
9	0	-1	-1	92.52	92.81
10	0	1	-1	97.30	97.48
11	0	-1	1	90.92	90.74
12	0	1	1	96.51	96.22
13	0	0	0	95.79	95.55
14	0	0	0	95.63	95.55
15	0	0	0	95.23	95.55

The coded independent variables and the experimental BBD matrix are listed in Table 3.10 along with the experimental and predicted values obtained for removal efficiency (Y_1). Table 3.11 summarize the results for analysis of variance (ANOVA) followed by Fisher's statistical test (F-test) for the experimental data obtained according to the BBD experiment. As one could see in Table 3.11, the ANOVA of the regression model shows that the quadratic model is highly significant, having a high value of the coefficient of determination R^2 (0.98956) indicating that 98.95% of the total variation is explained by this quadratic regression model. The high degree of adequacy of the quadratic model is also sustained by the Fisher's *F*-test (*F*model is 38.40) with a very low probability value (*P*model >*F* = 0.00043). The following equation, expressed in terms of coded variables, for removal efficiency (Y_1) was obtained by regression analysis:

$$Y_1 = 95.55303 + 0.18841X_1 - 0.11938X_1^2 + 2.53861X_2 - 1.04085X_2^2 - 0.83092X_3 - 0.19585X_3^2 - 0.0444X_1X_2 + 0.12083X_1X_3 + 0.20093X_2X_3 \qquad (3.92)$$

The values of p less than 0.05 from Table 13 indicate that the terms significant in model equation are the linear term X_3 and quadratic terms: $X_1^2$and X_2^2. All the other initial variables and interacting factors were not found to be statistically significant at 95% confidence limits.

Table 3.11 ANOVA test for response function Y_1 (removal efficiency)

Term	Sum of squares	DF	Mean square	F	p
Model	0.158619	9	0.017624	38.40290	0.000436[a]
X_1	0.28397	1	0.28397	2.1834	0.199555
X_2	0.05262	1	0.05262	0.4046	0.552701
X_3	51.55651	1	51.55651	396.3962	0.000006[a]
X_1^2	4.00010	1	4.00010	30.7551	0.002618[a]
X_2^2	5.52348	1	5.52348	42.4677	0.001272[a]
X_3^2	0.14163	1	0.14163	1.0890	0.344506
X_1X_2	0.00789	1	0.00789	0.0606	0.815289
X_1X_3	0.05840	1	0.05840	0.4490	0.532505
X_2X_3	0.16148	1	0.16148	1.2416	0.315841
Error	0.65032	5	0.28397	2.1834	0.199555
Total SS	62.29555	14			
R^2=0.98956	Adj R^2=0.97077				

[a] $P<0.05$ is considered significant

The fitted quadratic model simplified (terms statistically insignificant, based on p-values greater than 0.05, were omitted) is described by equation (3.93).

$$Y_1 = 95.55303 - 0.83092X_3 - 0.11938X_1^2 - 1.04085X_2^2 \quad (3.93)$$

These assumptions are also sustained by Pareto chart for the effects of process parameters, and of their interactions on the removal efficiency of Pb(II), presented in Fig. 3.12.

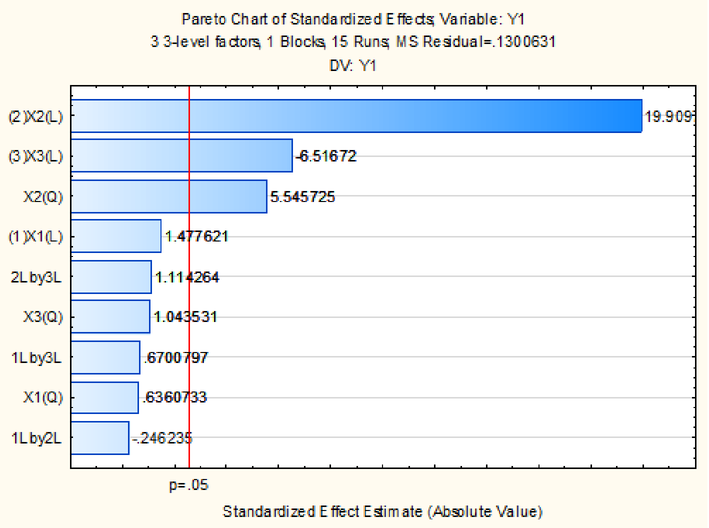

Figure 3.12 Paretto chart of main effects obtained from Box-Behnken factorial design

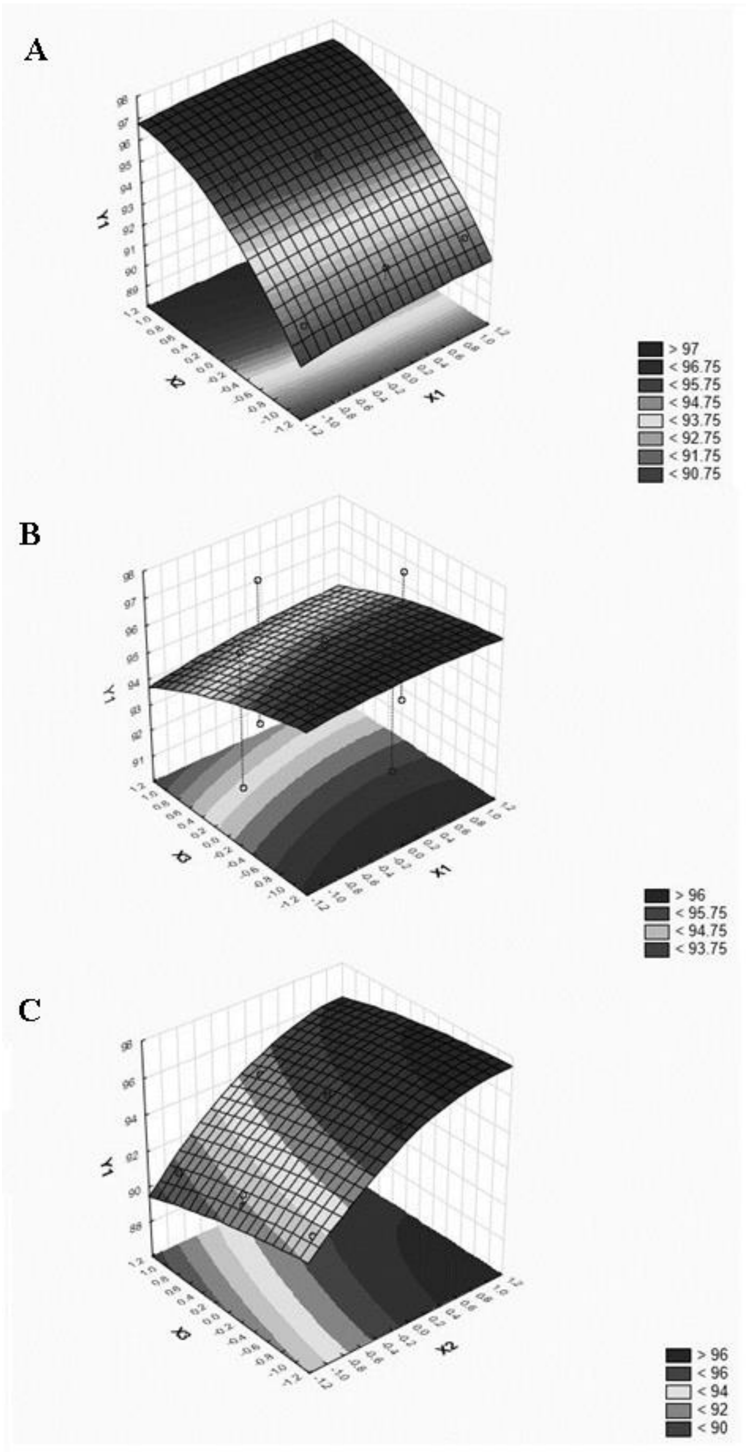

Figure 3.13 Response surface plots obtained from BBD for lead removal efficiency (Y_1) depending on (A) contact time (X_1) and initial Pb (II) concentration (X_2), (B) contact time (X_1) and temperature (X_3), (C) initial Pb (II) concentration (X_2) and temperature (X_3)

Response surface plot are also suitable to predict the Pb(II) removal efficiency. In Fig. 3.13 there are presented the response surface as a function of two variables while the third variable was kept constant at 0 coded values. From Fig. 3.13A one could see that the initial solution concentration is a very important factor for Pb(II) removal and so the maximum removal efficiency being obtained for X_2=1 as coded variable, that means a Pb (II) concentration of 80 mg/L. At lower concentration values the removal efficiency decreases. From Fig. 3.13B we observe that the surface plot indicates that both variables (working temperature and time) are not significant variables for the removal efficiency of Pb (II). Fig. 3.13C confirms the aforementioned conclusions, from the independent variables chosen, only initial Pb(II) concentration is the most important in determining the removal efficiency.

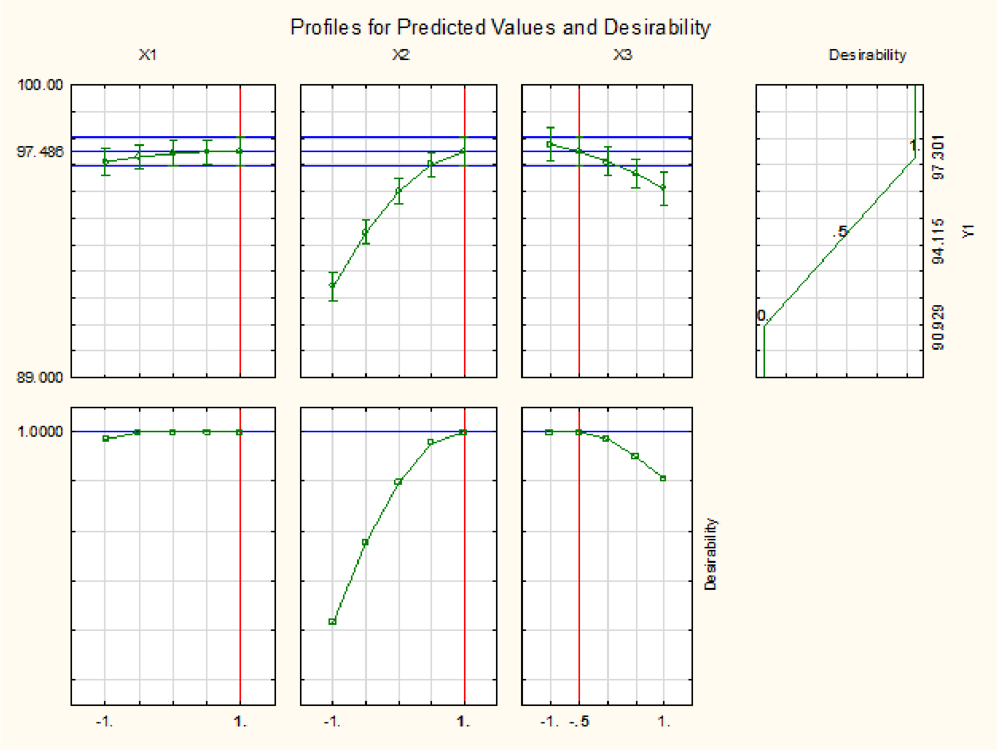

Figure 3.14. Profiles for predicted removal efficiency and the desirability level for different influencing factors for optimum US-AA of Pb(II) by HS

The desirability profiles were obtained using STATISTICA software and assigning predicted profiles to scale ranging from 0.0 (undesirable) to 1.0 (very desirables). For our experiments the desirability of 0 was assigned for minimum value of Y_1 (90.92) and the desirability of 1 was assigned for the maximum value of removal efficiency (Y_1=97.30). Based on the results depicted in Fig. 3.14 the coded values for each variables predicted to have a desirability score of 1 are: X_1=1, X_2=1 and X_3=-0.5, that means that the optimized model variables are: time 10 minutes, Pb (II) initial concentration 80 mg/L and working temperature 25 ºC. For these results validation new experiments (in duplicate) were done of the optimized variables values. The experimental results are in agreement with the data obtained from desirability optimization analysis.

Pb(II) adsorption on HS – US-AA equilibrium study: In a conservative approach, 20 min were considered necessary to attain equilibrium for all US-AA experiments. Conventional models, Langmuir and Freundlich were used to fit the experimental data for the initial concentration of Pb(II)solution ranging from 20 to 200 mg/L. The rest parameters were maintained at previously indicated optimal values. As can be seen in Figure3.15, Langmuir model describes better the US-AA process, with an acceptable correlation coefficient (R^2 around

95 %). According to this model, the maximum adsorption capacity (q_m) obtained is 147 mg/g, for the experiments at 20 ºC, showing a good adsorption capacity for of HS for Pb(II) in US-AA, comparable with other adsorbents, previously investigated (Sun et al., 2014).The value of <n> parameter in Freundlich isotherms, higher than 1.0, indicates the affinity of HS for Pb(II), not as high as for other adsorbents [61], but in the range of the obtained values for the HS in silent adsorption obtained by other researchers [64]. However, the correlation coefficient is lower, showing the unsuitability of this model for the interpretation of the experimental data.

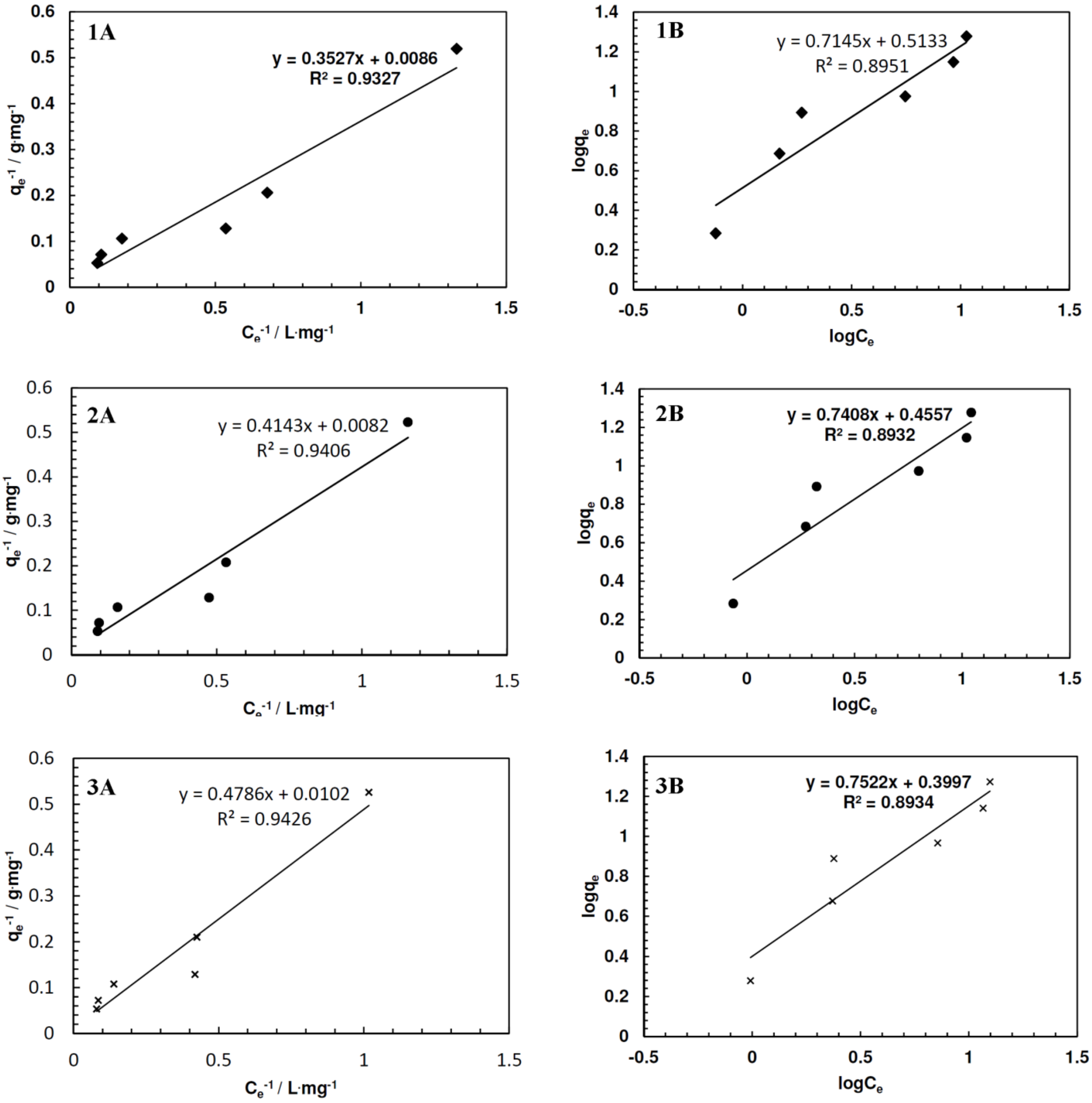

Figure 3.15 Langmuir (A - plots) and Freundlich (B - plots) adsorption isotherms for the US-AA of Pb(II); 1 – 20 ºC, 2 – 30 ºC, 3 – 40 ºC

4.2.5. Sorption dynamic experiments (116, Cap. 4)

Measurements of species sorption dynamics on HS was given of each of the two species and of the two species together. These were made as measurements to identify the sorption equilibrium but with a single concentration of species in liquid and by measuring the dynamic state of species concentration in liquid phase. First of all, these measurements were made when phases contacting occurs in absence of ultrasound. The working temperature was those characterizing the sorption isotherms, whereas the stirring rate and solid concentration in system was fixed at 180 rpm respectively 10 g/l. Several dynamics measurements were also performed in the presence of the ultrasound field

4.2.6. Modelling of experimental sorption dynamic (116-119, Cap.4)

The modelling of batch sorption dynamic for one or more components is a difficult problem due to number of parameters of equations and restrictions which describe the process [18 19]. Taking into account our experiments and more other from literature [18-23], we consider that at HS particle level, in its inside, the species (Pb(II) or/and Cd(II)) diffusion and their reaction with the HS sorbent sites control the sorption rate. In order to establish the correspondent mathematical model the following assumptions can be accepted: i) perfect mixing of liquid characterizes the flow of liquid phase; ii) the HS sorbent particles have a porous structure, a spherical shape with the same equivalent radius (*R*) and they are surrounded by a perfectly mixed liquid; iii) depending on experiment type the active molecules with Pb(II) or/and Cd(II) diffuse in solid particle pores, where these are adsorbed onto active surface sites; iv) overall adsorption rate of molecular species depends on the competition between adsorption and desorption processes; v) kinetics of sorption process is linear with respect to coverage degree of pores surface and species concentration in liquid phase; vi) kinetics of desorption process is linear with respect to species concentration in solid phase; vii) sorption experiments follow the isothermal process conditions. If we look to the phenomenological models from chapter 3 then we discover that our assumptions go to the model 3.3.2, with changing of nonlinear kinetic adsorption model with linear kinetic adsorption model. So, at particle level we have porous diffusion with linear kinetic adsorption model. According to the above considerations, the following system of equations and restrictions result. They express the process mathematical model for dynamic of simultaneous Pb(II) and Cd(II) sorption on HS.

-conservation of species of c_i concentration in the liquid from porous sorbent particle:

$$\frac{\partial c_i}{\partial \tau} = D_{ef,i}\left(\frac{\partial^2 \mathrm{c_i}}{\partial \mathrm{r}^2} + \frac{2}{r}\frac{\partial c_i}{\partial r}\right) - v_{Ri}(c_i, c_{si}) \tag{4.5}$$

- kinetic equation of species belonging to the solid phase (HS particle):

$$\frac{\rho_P}{\varepsilon_P}\frac{\partial c_{si}}{\partial \tau} = v_{Ri}(c_i, c_{si}) \tag{4.6}$$

- overall adsorption rate equation of considered species:

$$v_{Ri}(c_i, c_{si}) = k_{ai}\left(1 - \frac{\sum_{i=1}^{N} \alpha_i\, c_{si}}{Q}\right)c_i - k_{di}\frac{\rho_P}{\varepsilon_P}c_{si} \tag{4.7}$$

- balance of species transfer rate respect to solid phase (HS particle):

$$-V_l\frac{dc_{li}}{d\tau} = m_s\frac{dc_{si\,\mathrm{mn}}}{\mathrm{d}\tau} \tag{4.8}$$

- relationship for momentary mean concentration of *i* species in solid phase:

$$c_{si,mn}(\tau) = \frac{1}{R}\int_0^R c_{si}(r,\tau)dr \tag{4.9}$$

- initial conditions for solid and liquid species concentration field:

$$\begin{array}{lll} \tau = 0 & 0 \le \mathrm{r} < \mathrm{R} & \mathrm{c_i} = 0, \quad \mathrm{c_{si}} = 0 \\ \tau = 0 & r > R & c_{li} = c_{li0}, \end{array} \tag{4.10}$$

- boundary conditions for species diffusion (eq. (4.5)) in solid HS particle:

$$\begin{array}{lll} \tau > 0 & \mathrm{r} = 0 & \dfrac{\mathrm{dc_i}}{\mathrm{dr}} = 0, \quad \dfrac{\mathrm{dc_{si}}}{\mathrm{dr}} = 0 \\ \tau > 0 & r = R & V_l\dfrac{dc_{li}}{d\tau} = -D_{efi}S\left(\dfrac{dc_i}{d\tau}\right) \end{array} \tag{4.11}$$

The equations and restrictions system (4.5) - (4.11) were numerically transposed by an adequate finite differences method in a parameters identification problem, where values of momentary mean concentration of species in liquid phase $\{c_{li,(\tau)}\}$, depending on values of known parameters, namely R,ε_P , ρ_P, α_i,Q,c_{i0}, c_{li0} and unknown parameters $D_{ef,i}$, k_{ai}, k_{di}, are reported to the measured mean concentration of species in liquid phase. Minimizing the objective function described by equation (4.12), wherein $c_{li,exp}(\tau)$is experimental concentration ofi species in liquid phase at time τ_j, the values of $D_{ef,i}$, k_{ai} and k_{di} were identified.

$$f\left(D_{ef,i}, k_{ai}, k_{di}\right) = \sum_j \left[c_{li,mn}(\tau_j) - c_{li,\exp}(\tau_j)\right]^2 \tag{4.12}$$

It is important to show that from equilibrium data we can obtain an estimation for ratio of reaction constants of sorption and desorption processes. Also, from here is obtained the Q estimator for the total sorption capacity of the HS sorbent. If put in relation (4.7) the equilibrium condition and single species sorption the results is relation (4.4) with $a = \left(\frac{k_d}{k_a}\right)\left(\frac{\rho_p}{\epsilon}\right)$. For simultaneous sorbtion on HS when it put equilibrium conditions with relation (4.7) the result is in the system of equations (4.13) and (4.14), which can show values for Q, α_1,α_2, k_{d1}/k_{a1} and respectively k_{d2}/k_{a2}.

$$\frac{k_{d1}}{k_{a1}}\frac{\rho_p}{\varepsilon} = \left(1 - \frac{\alpha_1 c_{s1e} + \alpha_2 c_{s2e}}{Q}\right)\left(\frac{c_{l1e}}{c_{s1e}}\right) \tag{4.13}$$

$$\frac{k_{d2}}{k_{a1}}\frac{\rho_p}{\varepsilon} = \left(1 - \frac{\alpha_1 c_{s1e} + \alpha_2 c_{s2e}}{Q}\right)\left(\frac{c_{l2e}}{c_{s2e}}\right) \tag{4.14}$$

4.2.7 Results and discussions (125-128, Cap.4)

The third results of this research refers to sorption dynamics on HS sorbent of single or competitive Pb(II) and Cd (II), when the pH is established at 5.5, the solid liquid ratio correspond to 10 g/l and the HS particles diameter is fixed at 0.875 mm. Experimental data on sorption dynamics consisted in measuring of transferable species concentration in liquid phase, during an experiment. The data below specify what these measurements were, for all 6 cases investigated. In the case of single species sorption the algorithm for identifying the two parameters of the model (D_e and k_a because k_d comes from K_e and k_a) consisted in: i) numeric transposition of dynamic model ((4.5) - (4.11)) in its expression as a function showing species dynamic concentration in liquid $c_{lc}(D_e, k_a)$, ii) building the objective function (4.12) for parameters identifying based on experimental values c_{lex}, iii) minimizing of objective function after model parameters, iv) tabulating the identified parameters values; v) graphical representations of correspondence between experimental dynamics and model resulted and of model sensitivity towards the effective diffusion coefficient.

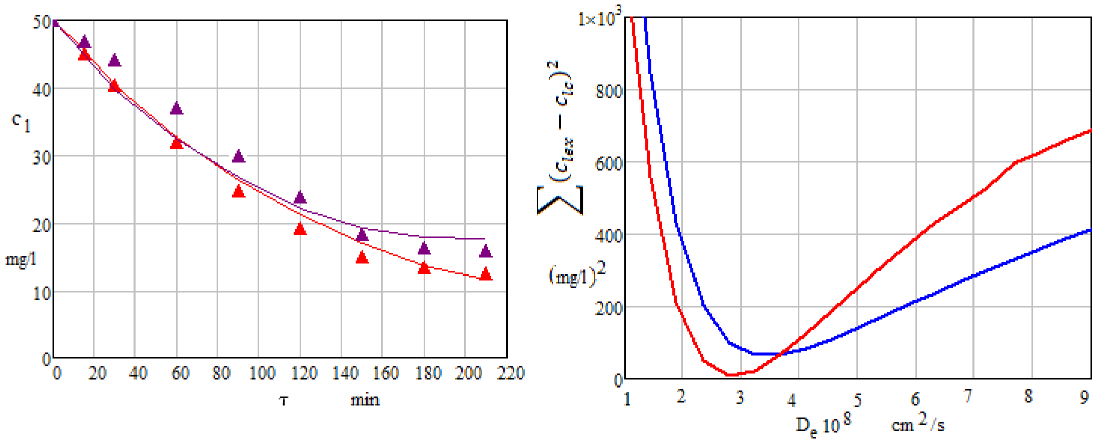

Figure 4.8 Dynamic of single Pb(II) and Cd(II) concentration in liquid (left) and sensibility of concentrations mean square deviation respect to diffusion coefficient (non US phases contacting; left: line- model data with parameters given in table 5, points –experimental data (red Pb(II), magenta Cd(II)); right –red Pb(II), blue Cd(II))

A similar procedure was used in the case of competitive sorption. In this case, instead of numeric function with two parameters, $c_{lc}(D_e, k_a)$, we have the equivalent function with four parameters, $c_{lc}(D_{e1}, k_{a1}, D_{e2}, k_{a2})$. It is not recommended to identify more than two parameters in a single data set [16]. Thus, for the competitive sorption, it was considered that the values of D_{e1}, k_{a1},D_{e2}, k_{a2} are close to those characterizing the single component sorption. You can find such values for these parameters that cover the experimental data well. Table 4.7 shows the identified values of dynamic model parameters, for all four experimentally investigated cases. Figure 4.8, by $c_l$vs τ dependence, experimental and according to the model, and by sensitivity of concentrations mean square deviation as a function of D_e, shows a good quality of parameters identifying, namely D_e and $k_a$at non-US single Pb (II) and Cd (II)sorption on HS. Figure 4.9 shows the same as figure 4.8, when phases contacting occurs in ultrasonic field. Experimental and model predicted $c_l$vs τ dependencies are given with figure 4.10. Left part of figure is c_l dynamics for Pb(II) and Cd(II)competitive sorption on HS without US field for time under 100 min. Right figure part shows this dynamic with US field presence.

Table 4.7 Identified values of dynamic model parameters (pH= 5.5, m_{HS} = 10 g/l, t = 25 ^{0}C)

Case	NoUS Pb(II)	NoUS Cd(II)	US Pb(II	US Cd(II)	NoUS Pb(II) Cd(II)	US Pb(II) Cd(II)
K_e	5.95 10^{-4}	6.58 10^{-4}	8.94 10^{-5}	7.62 10^{-4}	6.02 10^{-3} 8.11 10^{-3}	5.51 10^{-3}7.61 10^{-3}
k_a s^{-1}	2.91 10^{-4}	4.35 10^{-4}	4.05 10^{-3}	6.43 10^{-3}	9.05 10^{-5} 4.13 10^{-5}	3.01 10^{-4}2.25 10^{-4}
D_e m^2/s	2.9 10^{-8}	3.5 10^{-8}	6.4 10^{-7}	6.1 10^{-7}	1.5 10^{-8} 1.6 10^{-8}	6.3 10^{-7} 6.1 10^{-7}

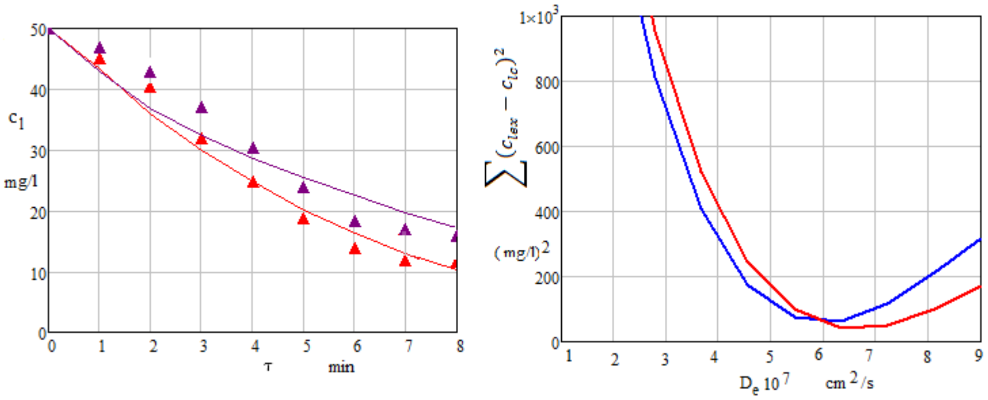

Figure 4.9 Dynamics of single Pb(II) and Cd(II) concentration in liquid (left) and sensibility of concentrations mean square deviation respect to diffusion coefficient (US phases contacting; left: line-model data with parameters given in table 5, points –experimental data (red Pb(II), magenta Cd(II)); right –red Pb(II), blue Cd(II))

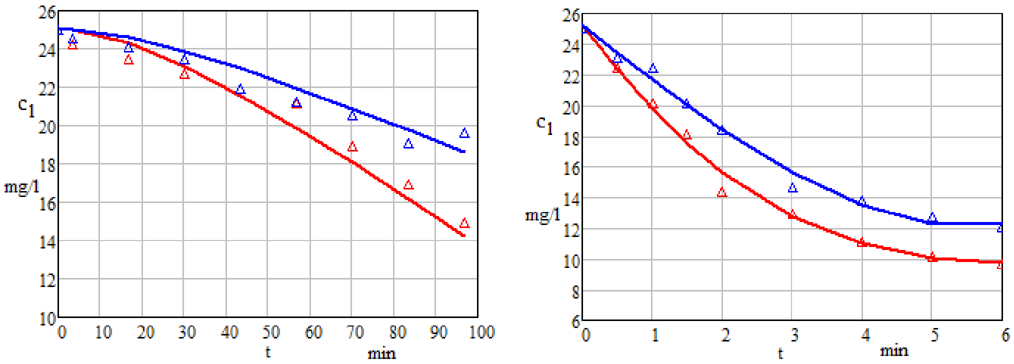

Figure 4.10 Dynamic of competitive Pb(II) and Cd(II) concentration in liquid for non US (left) and US (right) phases contacting (line: model with parameters given in table 5; points: experimental, red: Pb(II), blue Cd(II))

The above presented allow highlighting several aspects, of general and particular interest to the case. We show thus: i) the dynamics of the sorption in the ultrasonic field is almost 30 times faster than the one in its absence (fig. 4.8 compared with fig. 4.9 (left part of figures), respectively fig. 4.10 left and right part); ii) the fig 4.8, 4.9 and 4.10 show that the allure of sorption dynamics curves, from all 4 investigated cases, is the same; so it can be considered that whatever the case the process evolves similarly and so it can be characterized with the same model; iii) the diffusion coefficients for Pb (II) and Cd (II), at individual sorption, are, on average, 20 times higher in ultrasonic field (6.4 10^{-7} respectively 6.1 10^{-7}) operation than in its absence (2.9 10^{-8} respectively 3.5 10^{-8}); iv) given the structural proximity between Pb (II) and Cd (II) species, their diffusion coefficients in HS, whatever the sorption procedure, are very close, as shown in the last line of Table 4.7: v) the interaction between Pb (II) and Cd (II) in competitive non US sorption has concretely proof in differences, of almost 2.5 times, between the individual diffusion coefficients in HS and those corresponding to the simultaneous diffusion (values from last line in table 4.7 columns 2 and 4 compared with values from the same line column 6); vi) in US phases contacting the effect of species interaction on competitive sorption does not appear to be significant (values from the last line columns 4 and 5 not differ from those from the same line column 7); vii) the values of diffusion coefficient for Pb(II) and Cd(II) in HS vegetal structure correspond with some other published [39-41] and are in the range of ionic species diffusion in mean hard structured sorbents [42]; viii) along with the differentiation given by the diffusion coefficient, the large difference between the speed of the sorption process in the presence of the US and that in the absence of the US is also supported by the strong differentiation of the constant k_a of the sorption rate; we thus find for single sorption k_{aUSPb}/k_{aNUSPb}= 13.92 (table 4.7: value line 3 column 4 compared with value line 3 column 2), k_{aUSCd}/k_{aNUSCd}= 14.78 (table 4.7: value line 3 column 5 compared with value line 3 column 3) respectively k_{aUSPb}/k_{aNUSPb} = 3.35

and k_{aUSCd}/k_{aNUSCd}= 5.44 (ratio computed with values from table 4.7 line 3 column 7 and 6) in competitive sorption; ix) comparing the values of the adsorption rate constants (table 4.7 line 3) as well the ratios of these constants given above it is appreciated that in the competitive sorption the species concurrence for the most of sorption sites makes their occupation frequency less than when competition is lacking (table 4.7: $9.05\ 10^{-5}<2.910^{-4}$; $4.13\ 10^{-5}<4.34\ 10^{-4}$, $3.01\ 10^{-4}<4.05\ 10^{-3}$, $2.25\ 10^{-4}<6.43\ 10^{-3}$). The ones presented confirm that the model of sorption dynamics of species Pb(II) and Cd(II) on HS is adequate. It was thus possible to identify the diffusion coefficients of Pb(II) and Cd(II) species as well as the coefficients of the sorption and desorption rates of these species in their interaction with the HS plant structure, in the absence or presence of the US field.

5.3.2 Modeling of simultaneous Pb(II) and Cd(II) sorption in HS fixed bed (143-145 Cap. 5)

It can be deduced from what we showed in Chapter 3 that when the species Pb(II) and Cd(II) are simultaneously retained in a fixed bed, four partly differential equations give the process evolution at particle level [31, 32]. Considering the values of the diffusion coefficients of the Pb(II) and Cd(II) species in HS particle (table 3.5, Chapter 3), the partly differential equations for concentration field in the particle should be 2D. As the flow also introduces the spatial coordinate, it results that the complete model process must be 3D. But if it is accepted that having small particles we can neglect the diffusion in them, then the equations of the sorption model can be written in 2D, showing changes according to z and τ. In this case we can consider the following assumptions about the process evolution: a) The net rate at particle level is a competition between the species sorption and desorption, depending on the occupation degree of active sites of sorbent. b) Linear combined models are acceptable for sorption and desorption processes rates. c) Plug flow with axial dispersion characterizes the liquid flow in the bed. With these conditions the process mathematical model is described by mean of the following relationships assembly:

- conservation relationships for ions species flowing with the liquid in the bed:

$$\frac{\partial c_i}{\partial \tau}+v\frac{\partial c_i}{\partial z}=D_l\frac{\partial^2 c_i}{\partial z^2}-v_{si}(c_j,s_j)\text{ , i = Pb(II),}\,Cd(II);\text{ j}=Pb(II)\ and\ Cd(II) \qquad (5.21)$$

- equations showing the species net sorption rate:

$$v_{si}(c_j,s_j)=k_{ai}\left(1-\frac{\sum_j a_{ij}s_j}{Q_i}\right)c_i-k_{di}s_i\text{ , i = Pb(II),}\,Cd(II);\text{ j}=Pb(II)\ and\ Cd(II) \qquad (5.22)$$

- conservation equations which give the accumulation of Pb(II) andCd(II) in particle:

$$\frac{\partial s_i}{\partial \tau} = v_{si}(c_j, s_j), \mathrm{i} = \mathrm{Pb(II)}, Cd(II);\ \mathrm{j} = Pb(II)\ and\ Cd(II) \qquad (5.23)$$

- univocity conditions for the above partly differential equations:

$$\tau = 0,\ 0 < \mathrm{z} < \mathrm{H},\ \mathrm{c_j} = 0, \mathrm{s_j} = 0,\ \mathrm{j} = Pb(II)\ and\ Cd(II) \qquad (5.24)$$

$$\tau > 0,\ \mathrm{z} = 0,\ \mathrm{c_j} = c_{j0},\ \mathrm{j} = Pb(II)\ and\ Cd(II\ ) \qquad (5.25)$$

$$\tau > 0,\ 0 < \mathrm{z} < \mathrm{h},\ \mathrm{c_j} \le c_{j0},\ s_j \le s_j^*,\ \mathrm{j} = Pb(II)\ and\ Cd(II)^- \qquad (5.26)$$

$$\tau > 0, \mathrm{z} = \mathrm{H},\ \frac{\mathrm{dc_j}}{\mathrm{dz}} = -\frac{v}{D_l}(c_j - c_{jex}),\ \mathrm{j} = Pb(II)\ and\ Cd(II) \qquad (5.27)$$

The analyze of model formed by the ensemble of relations (5.21) – (5.27), shows that it is possible to numerically it integrated because: i) The flow velocity in the layer *v* can be calculated knowing the flow rate (1.4 ml/s) the flow section through the layer (3.14 cm^2). ii) The axial dispersion coefficient $D_l$is expressed from $Pe_d = 2$. iii) The kinetic constants of sorption and desorption for species participating in sorption are taken from table 5.5, which is a selection from table 5.5, Chapter 4.

Table 5.5 Equilibrium constant and sorption process constant at single and competitive sorption of Pb(II) and Cd(II) onto HS (t= 250C, c0 = 50 mg/l)

Case	NoUS Pb(II)	NoUS Cd(II)	NoUS Pb(II) Cd(II)
K_e	$5.95\ 10^{-4}$	$6.58\ 10^{-4}$	$6.02\ 10^{-3}$ $8.11\ 10^{-3}$
k_a s^{-1}	$2.91\ 10^{-4}$	$4.35\ 10^{-4}$	$9.05\,0^{-5}$ $4.13\ 10^{-5}$

5.3.3 Results from numerical model integration(145 – 146, Cap. 5)

A numerical integration program with 20 integration steps along z, from 0 to h, and 1000 time sequences of 18 s/sequence allowed the generation of the 4 matrices that give the spatiotemporal dynamics of Pb(II) and Cd(II) in solid fixed bed and in the liquid flowing through the bed. It was thus possible to extract the breakthrough curve and goes to it compare with the one given in the figure 5.8.

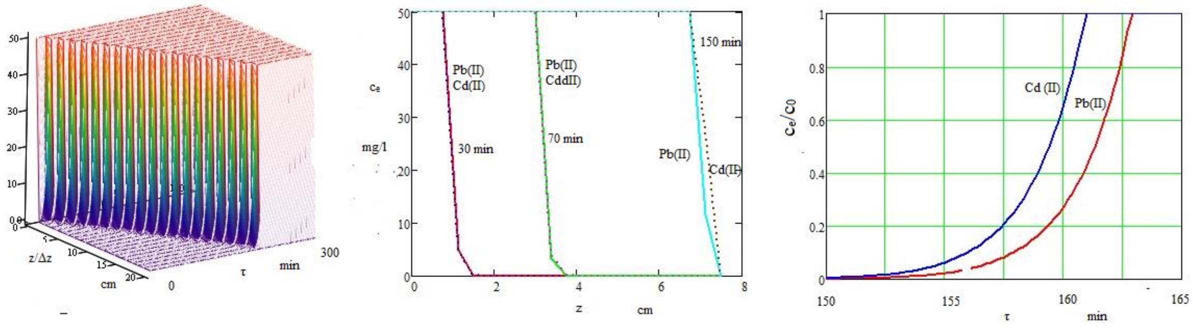

Figure 5.9 Simulation of fixed bed sorption of Pb(II) and Cd(II) with model (5.21) – (5.27)

(3D dynamics (left), 2D dynamics at selected time (center), breakthrough curve (right), t = 25 °C, v = 0.011 cm/s, Dl = 0.0055 cm^2/s, $k_{aPb(II)}$, $k_{dPb(II)}$, $k_{aCd(II)}$, $k_{dCd(II)}$ -according to table 5.5)

The results of concrete case simulation of the simultaneous removal in a fixed bed from HS of Pb(II) and Cd(II) are concentrated in figure 5.9. In the first one, the ones presented show us the penetration capacity in the process with the help of the model, that is, we can see what happens in layer in any position and at any moment (3D representation) or we can choose to see the state of transferable species, Pb(II) and Cd(II), concentration along the bed at selected time moments (2D representation) and obviously we can had the breakthrough curve. Secondly, we can choose any simulation situation we want, as it is shown in figure 5.10, where the effect of reducing the liquid flow velocity in the bed was simulated by half compared to the one considered in figure 5.9. Thirdly, by comparing the simulation with the experimental data, we can validate or not the model or rather the values of the parameters used in the simulation of the model.

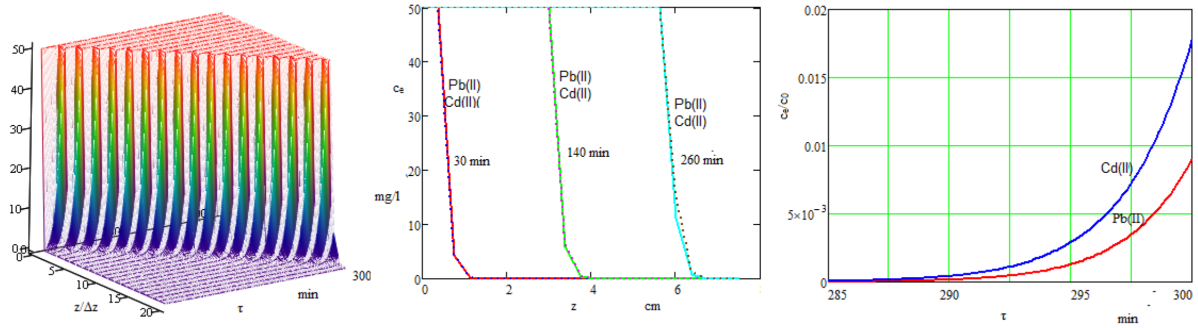

Figure 5.10 Effect of liquid velocity at simulation of fixed bed sorption of Pb(II) and Cd(II) by model (5.21) – (5.27), (3D dynamics (left), 2D dynamics at selected time (center), breakthrough curve (right), t = 25 °C, v = 0.005 cm/s, Dl = 0.0055 cm^2/s, $k_{aPb(II)}$, $k_{dPb(II)}$, $k_{aCd(II)}$, $k_{dCd(II)}$ -according to table 5.5)

Unfortunately, comparing those from figure 5.9 with those from figure 5.8, we find that: a) some approximation between the starting position of the experimental and theoretical curves in the sense that the experimental ones start at around time of 80 min and end at time 170 minutes and the theoretical one's finish at time 170 minutes; b) a strong bias in terms of the time width of these experimental curves, being much wider. We can thus appreciate that we cannot neglect the diffusion of species in the pores of particles. And normally, as we shown in Chapter 4, the diffusion that is accompanied by sorption and desorption. In other words, the process is in the pores and less on the surface of the particles.

6. General conclusions and perspectives (150-152, Cap. 6)

The thesis focuses on the problem of promoting of sorption processes with sorbents from natural products as application for removing heavy metals from wastewater. In this sense the thesis contains data, structured information, own points view regarding the pollution of water, soil and air with heavy metals (HM) and, respectively, its control primarily through sorption with sorbents from vegetable materials (biosorbents). The thesis red thread is that of the most complete characterization of sorption of Pb(II) and Cd(II), from wastewater, on the sorbent from particles from processed hazelnut shells (HS). The sorption enhancement, of the two species by the HS sorbent, through the use of the ultrasonic field is part of the previously mentioned red thread. Taking into account the doctoral theses custom of, we present here, with reference to each thesis chapter, those that are appreciated as their own contribution to the general and particular issues of the developed problem.

Respect to first thesis Chapter *Heavy Metal Pollution and General Methods for It Control* we show that we managed to show how we are doing with the application of sorption methods to this problem. On the other hand, the choice of the paragraphs for the development of the chapter and especially the content elements brought in them can claim that this chapter has elements of originality. In this sense it is mentioned: i) It was insisted on the positioning of heavy metals in the Mendeleev table in order to classify them, with literature and own elements (table 1.1), in three danger classes for man and environment. ii) Was made a classification of sources for environmental discharge of pollutants based on HM and this classification was exemplified. iii) The problem of processing of HM polluted water has sufficiently developed, with a strong emphasis on technology of hydroxides or sulphides HM precipitation. iv) It was noted that in the depollution of HM contaminated soils by using of crops with high capacity for HM fixing is modern and of interest, especially since it can be supported by genetic intervention on plants that form such crops. v) It has been shown that air pollution with HM is a consequence of its pollution with PM and that a great responsibility related to this pollution has the road transport based on fossil fuels. vi) In HM pollution control the biosorption and bioaccumulation are recommended as novel, efficient, eco-friendly, and less costly alternative technologies over the conventional methods.

The second Chapter, *Adsorption and Biosorption Processing of Heavy Metals Polluted Water*, between more other elements of high interest, contains data and processed information about the adsorption equilibrium when contacting HM wastewater with a sorbent. Also here is developed an experimental and modelling investigation regarding the characterization of the sorption equilibrium for Pb(II) and Cd(II) in the fixed bed contacting of wastewater with these pollutants and the sorbent from HS particles. As aspects that show the own elements of information organization and originality, the following are mentioned: i) For monocomponent sorption, a systematic presentation of the interphase equilibrium models was made with the specification of the experimental solutions for their parameters'identification and with concrete particularization to HM adsorption, from wastewater, on/in biosorbents. ii) The difficulty of putting in work of equilibrium models for multicomponent adsorption was shown and cases of simultaneous HM adsorption on biosorbents were commented. iii) All conditions for experimental investigation and experimental data processing were achieved, in order to identify the Langmuir and Freundlich equilibrium models parameters at individual adsorption, in a fixed bed, of Pb(II) and Cd(II) on the HS sorbent. iv) The experimental data of simultaneous equilibrium adsorption for Pb(II) and Cd(II) were exploited by developing a new procedure in which the equilibrium results from individual adsorption are used.

The Chapter 3 *Modelling of Heavy Metals Adsorption in Wastewater Depollution* begins by focusing on presentation of phenomenological models specific to species, including species based on heavy metals, adsorption on selected sorbent. But the complexity of phenomenological models has oriented research from this area towards the use of statistical models, most often based on the programming of experiences. Thus, the paragraph 3.5, completely original, is dedicated to the use of a statistical model for characterizing ultrasonic adsorption of Pb (II) on hazelnut shell particles. From this investigation the conclusions are presented as follows: i) Was proved, one more time, that HS can be used as low cost adsorbent for Pb(II) with no major modifications. ii) The statistical response surface model (RSM), based on three factors, three levels BBD, was successfully implemented to allow optimization of operating parameters and the obtained results show good potential applicability of this combined technique at industrial scale. iii) In different approaches, it was found that the combination of adsorption with ultrasound power determined a significant decrease of necessary contacting time to obtain very good removal efficiency. iv) The obtained results could be the base for further investigations with the purpose of obtaining very low levels of Pb(II) in treated wastewater, to achieve guideline values and in this sense the factors to be investigated should be ones directly related to US (power, amplitude, etc.).

In Chapter 4 *Models at Particle Level in Adsorption of Heavy Metals on Vegetable Sorbents*, for the case study named Ultrasound assisted competitive removal of lead and cadmium: statistic and dynamic models' development was chosen two modelling ways**.** The purpose of this choosing consists in explaining and highlighting of a big experimental data volume concerning eight investigated cases: a) Single Pb(II) and Cd(II) batch sorption on HS with and without US (4 cases). b) Competitive Pb(II) and Cd(II) batch sorption on HS with and without US (4 cases). Stochastic modelling was used to shows the dependence of equilibrium species sorption efficiency upon HS particle diameter, liquid solution pH, solid/liquid ratio, and initial species concentration in liquid phase. Respect to relevant aspects of Pb(II) and Cd(II) adsorption statics on HS it shows that: i) Liquid-solid (HS) equilibrium for single Pb(II) and Cd(II) was modelled via Langmuir model. ii) A new procedure was applied for elevation of equilibrium isotherms of competitive sorption of Pb(II) and Cd(II) in US and non US field. iii) The obtained equilibrium results find of those presented at the Chapter 2. For dynamics of the sorption process is considered the complex model of unsteady diffusion with competitive sorption and desorption in solid particles. In this problem we show that: i) The building of numerical form of model as a function having effective diffusion coefficient and the desorption rate constant as argument, becomes possible the identifying of these parameters. ii) The numerical model working is based on experimental curves that give the dynamics of the liquid concentration of the transferable species, Pb (II), Cd (II) respectively Pb (II) and Cd (II), either in non-US or in US phases contacting. iii) We appreciate that **we publish for the first time** values for effective diffusion coefficients and sorption rate coefficients at contacting of vegetal sorbent (HS particles) with wastewater with HM (Pb(II) and Cd(II)) in ultrasonic field.

In opening of chapter 5 *Adsorption of Heavy Metals in Sorbent Fixed Bed* it shows that is important, for a given fixed bed sorption case, the determining of fixed bed optimal volume. The considered model for calculating of the sorbent fixed bed volume requires an expression, from experimental or modeling breakthrough curves, of dependence of current adsorption operating time versus fixed bed sorbent volume. In this sense, for our problem of Pb(II) and Cd(II) removal in fixed bed of HS particle, the following were undertaken: i) Was obtained the experimental elevation of the breakthrough curves for the adsorption of Pb(II) and Cd(II) from waste water, in a fixed layer of HS. ii) It turned out that both breakthrough curves, of the HS fixed bed in the case of Pb(II) and Cd(II), can be characterized with semi-empirical models such as the Thomas model and Hutchins's BDSF model. iii) Based on the experimental data, these models' parameters are identified so that they can be used to express the above-mentioned dependence. iv) When the species Pb(II) and Cd(II) are simultaneously retained in a fixed bed, four partly differential equations give the process evolution at particle level; a 2D simplified model was considered for this case. v) Even if it was not possible for 2D model to be validated by experimental data for simultaneous Pb(II) and Cd(II) adsorption, it shows that the power to penetrate the process with simulation help is important and recommended to be used.

In one way or another, any scientific work open, on the same basis, new research directions. Concretely, we consider that we can recommend:

A. Promotion of high efficiency working methods in the sense of mass transfer enhancement through innovative solutions for phases contacting, respectively by intelligent modification of the sorbents (we obtained, when operating in the ultrasonic field, times to reach the equilibrium less than 10 minutes compared to those classics over 200 minutes).

B. The development of integrated solutions in which the process of removing of HM pollutants from wastewater should consider the pre-processing of the sorbent and its post-process separation.
C. Supporting management research regarding the management of sorbents in the sense of clearly defining of methods of their use and release in an applied industrial process
D. Moving as far as possible from biosorption of HM from wastewater to bioremediation of wastewater containing HM.

References:

Chapter 1

10. S. Rengaraj, S. Moon,Kinetics of adsorption of Co(II) removal from water and wastewater by ion exchange resins, *Water Res*., 36, 2002, 1783-1793.

11. J. S. Kim, M. A. Keane,The removal of iron and cobalt from aqueous solutions by ion exchange with Na-Y zeolite: batch, semi-batch and continuous operation, *J. Chem. Technol. Biot*., 77), 2002, 633-640.

12. M. A. Al-Ghouti, M. A. M. Khraisheh, M. Tutuji,Flow injection potentiometric stripping analysis for study of adsorption of heavy metal ions onto modified diatomite, *Chem. Eng.* J., 104, 2004, 83-91.

13. R. A. Goyer, Toxic effects of metals. In: Casarett and Doull's Toxicology: *The Basic Science of Poisons,* 6th Ed., McGraw-Hill, 2001, 817-823.

14. US EPA, Office of Water 4606M, EPA 816-F-03-016 *National Primary Drinking* Water Standards, June, 2003.

15. World Health Organization, *Guidelines for drinking-water quality*: 4th Ed., ISBN 978 92 4 154815 1, 2011.

16. Davis A., Volesky B.,Vierra R., Sargassum Seaweed as Biosorbent for Heavy Metals, *Water Res*., 34, 17, 4270-4278, 2000

Chapter 2

117. Ahmed S. B., Dobre T., Kamar F. H., Deleanu Iuliana, Biosorption of Lead and Cadmium onto Hazelnuts Shells in a Fxed Bed Column, *U.P.B Sci. Bull. Series C*, 84 (3) 2022.

118. Pindiga N. Y., Walid A. H., Abdullahi A. O., Mohammad A.B., Kinetic, Equilibrium and Thermodynamic Study of the Adsorption of Pb (II) and Cd (II) Ions from Aqueous Solution by the Leaves Biomass of Guava and Cashew Plants, *Online Journal of Chemistry*, *2,* 1, 23–38, 2022.

Chapter 3

47. Bdaiwi Ahmed S., Stoica-Guzun A., Kamar F. H., Dobre T., Gudovan D., Busuioc C., Jipa I. M., Ultrasound enhanced removal of lead from wastewater by hazelnut shell: an experimental design methodology, *International Journal of Environmental Science and Technology*, 5, 123-134, 2018, DOI:10.1007/s13762-018-1782-z.

48. Henze M., Comeau Y., Wastewater Characterization. In: Henze M., van Loosdrecht M.C.M., Ekama G.A., Brdjanovic D (eds) Biological Wastewater Treatment: Principles, Modelling and Design, *IWA Publishing*, London, UK, 33-52(2008).

49. Madala S, Reddy M.V.N., Vudagandla S., Abburi K., Modified leaf biomass for Pb(II) removal from aqueous solution: Application of response surface methodology,EcolEng 83:. 218-226, 2015, DOI: 10.1016/j.ecoleng.2015.06.025.

50. Matlock M.M., Howerton B.S., Atwood D.A.,) Irreversible precipitation of mercury and lead. *J. Hazard Mater.*, 84, 1, 73-82, 2001, DOI.org/10.1016/S0304-3894(01)00190-X.

51. Hubadillah S. K., Othman M.H.D., Harun Z., Ismail A.F., Rahman M.A., Jaafar J., A novel green ceramic hollow fiber membrane (CHFM) derived from rice husk ash as combined adsorbent-separator for efficient heavy metals removal, *Ceram Int.*, 43, 5, 4716-4720, 2017), DOI.org/10.1016/j.ceramint.2016.12.122.

52. Kumari A.R., Sobha K., Removal of lead by adsorption with the renewable biopolymer composite of feather (Dromaius novaehollandiae) and chitosan (Agaricusbisporus). *Enviro. Technol. Innovations*, 6, 11-26, 2016, DOI.org/10.1016/j.eti.2016.04.004.

53. Harja M., Buema G., Sutiman D.M., Cretescu I., Removal of heavy metal ions from aqueous solutions using low-cost sorbents obtained from ash,*Chem Pap.*, 67, 5, 497-508, 2013, DOI: 10.2478/s11696-012-0303-7.

54. Saka C, Sahin O, Kucuk MM (2012) Applications on agricultural and forest waste adsorbentsfor the removal of lead (II) from contaminated waters. *Int..J Environ.Sci.Technol.*, 9, 379-394, 2012,DOI 10.1007/s13762-012-0041-y.

55. Bulgariu L., Bulgariu D., Macoveanu M.,) Characteristics of sorption of uncomplexed and complexed Pb(II) from aqueous solutions onto peat, Chem Pap., 66, 4, 239-247, 2012, DOI: 10.2478/s11696-012-0149-z.

55. Bayrak Y., Yesiloglu Y., Gecgel U., Adsorption behavior of Cr (VI) on activated hazelnut shell ash and activated bentonite, *Micropor.Mesopor.Mat.*, 91, 107-110, 2006, DOI: 10.1016/j.micromeso.2005.11.010.

56. Pehlivan E., Altun T., Cetin S., Bhanger M.I.,) Lead sorption by waste biomass of hazelnut and almond shell, *J. Hazard. Mater.*,167, 1203-1208, 2009, DOI: 10.1016/j.jhazmat.2009.01.126.

57. Ferrero F., Dye removal by low-cost adsorbents: Hazelnut shells in comparison with wood sawdust. J. Hazard. Mater., 142,144-152, 200,DOI: 10.1016/j.jhazmat.2006.07.072.

58. Dogan M., Abak H., Alkan M., Adsorption of methylene blue onto hazelnut shell: Kinetics, mechanism and activation parameters. *J. Hazard. Mater.*, 164,172-181,2009, DOI:10.1016/j.jhazmat.2008.07.155.

59. Stoica-Guzun A, Stroescu M, Jinga S.I., Mihalache N., Botez A., Matei C., Berger D., Damian C.M., Ionita V., Box-Behnken experimental design for chromium (VI) ions removal by bacterial cellulose-magnetite composites, *Int. J. Biol. Macromolec.*, 91, 1062-1072, 2016.

60. Sun S., Yang J., Li Y,, Wang K., Li X., Optimizing adsorption of Pb(II) by modified litchi pericarp using the response surface methodology, Ecotoxicol. . Saf., 108, 29-35, 2014.

61. Bakisgan C., Dumanli A.G., Yurum Y., Trace elements in Turkish biomass fuels: Ashes of wheat straw, olive bagasse and hazelnut shell, *Fuel* 88, 1842-1851,2009.

62. Haykiri-Acma H., Yaman S., Kucukbayrak S., Combustion characteristics of sodium-free pyrolytic char from hazelnut shell, *Fuel Process Technol*., 96, 169–174, 2012.

63. Pehlivan E., Altun T., Cetin S., Bhanger M.I., Lead sorption by waste biomass of hazelnut and almond shell, *J. Hazard Mater*., 167, 1203-1208. 2009.

64. Yadanaparthi S.K.R., Graybill D., von Wandruszka R., Adsorbents for the removal of arsenic, cadmium, and lead from contaminated waters. *J Hazard Mater* 171, 1-15. 2009.

65. Dil E,A., Ghaedi M., Asfaram A., Hajati S., Mehrabi F., Goudarzi A., Preparation of nanomaterials for the ultrasound-enhanced removal of Pb^{2+} ions and malachite green dye: Chemometric optimization and modeling. *Ultrason Sonochem*, 34, 677-691, 2017.

66. Pehlivan E., Arslan G., Removal of metal ions using lignite in aqueous solution low cost biosorbents. *Fuel Process. Technol.* 88, 99–106, 2007.

67. Zare-Dorabei R., Ferdowsi S.M,, Barzin A., Tadjarodi A., Highly efficient simultaneous ultrasonic-assisted adsorption of Pb(II), Cd(II), Ni(II) and Cu (II) ions from aqueous solutions by graphene oxide modified with 2,20-dipyridylamine: Central composite design optimization, *Ultrason Sonochem* 32, 265-276. 2016.

Chapter 4

18. T.Dobre, J.M Sanchez, Chemical engineering modelling simulation and similitude, Chapter 3 Mathematical models based on transport phenomena, Chapter 5 Statistical Modeling, *Wiley VCH*, 2007

19. R. Aris, Interpretation of sorption and diffusion data in poros solids, *Ind. Engng. Chem. Fundam.* 22, 150-151, 1983

20.D.D. Do, R.G. Rice, On the relative importance of pore and surface diffusion in non-equilibrum adsorption rate processes, *Chem. Eng. Sci*., 42, 10, 2269-2284, 1987

21. J. F Kelly, O. M Fuller, An evaluation of a method for investigating sorption and diffusion in porous solids, *Ind.Engng.Chem.Fundam*., 19, 11-17, 1980

22. Z. Reddad, C. Gerente, Y. Andres, P. L. Cloirec, Adsorption of several metal ions onto a low-cost biosorbent: Kinetic and equilibrium studies, *Environ. Sci. Technol.*, 36, 2067-2074, 2002

23. O. Dima, T.Dobre, Mathematical modeling and simulation of adsorption process in a fixed bed of molecularly imprinted polymeric pearls, *UPB Scientific Bulletin, Series B: Chemistry and Materials Science*, 78, 2, 143-154, 2016

24. A. Verma, M. Agarwal, S. Sharma, N. Singh, Competitive removal of cadmium and lead ions from synthetic wastewater using Kappaphycus striatum, *Environ. Nanotechnology*, Monit. Manag. 15 (2021) 100449. https://doi.org/10.1016/j.enmm.2021.100449.

Chapter 5

29. T.C. Egbosiuba, M.C. Egwunyenga, J.O. Tijani, S. Mustapha, A.S. Abdulkareem, A.S. Kovo, V. Krikstolaityte, A. Veksha, M. Wagner, G. Lisak, Activated multi-walled carbon nanotubes decorated with zero valent nickel nanoparticles for arsenic, cadmium and lead adsorption from wastewater in a batch and continuous flow modes, *J. Hazard. Mater.* 423 (2022) 126993. https://doi.org/10.1016/j.jhazmat.2021.126993.

30. V.C. Taty-Costodes, H. Fauduet, C. Porte, Y.S. Ho, Removal of lead (II) ions from synthetic and real effluents using immobilized Pinus sylvestris sawdust: Adsorption on a fixed-bed column, *J. Hazard. Mater.* 123 (2005) 135–144. https://doi.org/10.1016/j.jhazmat.2005.03.032.

31. DePaoli S. M., Perona J.J., Model for Sr-Cs-Ca-Mg-Na Ion-Exchange Uptake Kinetics on Chabazite, *AIChE J.,*42, 3434-3441, 1996.

32. Dobre T, Calotă L., Pârvulescu, O. C., Iavorschi G., Use of Experimental Breakthrough Curves for Ion Exchange Process Optimization, *U.P.B. Sci. Bull.,* 68, 4, 13-26, 200.